Cell Tissue Res (2015) 359:441–451
DOI 10.1007/s00441-014-2051-1

REGULAR ARTICLE

Sympathetic and sensory innervation of small intensely fluorescent (SIF) cells in rat superior cervical ganglion

Fumiya Takaki · Nobuaki Nakamuta · Tatsumi Kusakabe · Yoshio Yamamoto

Received: 2 September 2014 / Accepted: 3 November 2014 / Published online: 23 November 2014

Abstract The sympathetic ganglion contains small intensely fluorescent (SIF) cells derived from the neural crest. We morphologically characterize SIF cells and focus on their relationship with ganglionic cells, preganglionic nerve fibers and sensory nerve endings. SIF cells stained intensely for tyrosine hydroxylase (TH), with a few cells also being immunoreactive for dopamine β-hydroxylase (DBH). Vesicular acetylcholine transporter (VAChT)-immunoreactive puncta were distributed around some clusters of SIF cells, whereas some SIF cells closely abutted DBH-immunoreactive ganglionic cells. SIF cells contained bassoon-immunoreactive products beneath the cell membrane at the attachments and on opposite sites to the ganglionic cells. Ganglion neurons and SIF cells were immunoreactive to dopamine D2 receptors. Immunohistochemistry for P2X3 revealed ramified nerve endings with P2X3 immunoreactivity around SIF cells. Triple-labeling for P2X3, TH and VAChT allowed the classification of SIF cells into three types based on their innervation: (1) with only VAChT-immunoreactive puncta, (2) with only P2X3-immunoreactive nerve endings, (3) with both P2X3-immunoreactive nerve endings and VAChT-immunoreactive puncta. The results of retrograde tracing with fast blue dye indicated that most of these nerve endings originated from the petrosal ganglion. Thus, SIF cells in the superior cervical ganglion are innervated by preganglionic fibers and glossopharyngeal sensory nerve endings and can be classified into three types. SIF cells might modulate sympathetic activity in the superior cervical ganglion.

Keywords Sympathetic ganglion · Superior cervical ganglion · Small intensely fluorescent cells · Interneuron · Sensory nerve ending · P2X3 purinoreceptor · Paraganglionic cells · Rat (Wistar)

Introduction

The sympathetic ganglion contains small intensely fluorescent (SIF) cells (derived from the neural crest) and sympathetic ganglionic cells (Eränkö 1978; Matthews 1989; Huber 2006; Shtukmaster et al. 2013) and has been shown to be immunoreactive for tyrosine hydroxylase (TH) and/or dopamine β-hydroxylase (DBH; Borghini et al. 1994; Heym et al. 1993, 1994; Prud'homme et al. 1999). Electron microscopy has revealed that SIF cells contain numerous dense-core vesicles and make afferent synapses with preganglionic sympathetic nerve terminals and efferent synapses with the dendrites of postganglionic neurons (Kondo 1977; Matthews and Raisman 1969; Case and Matthews 1985). Physiological studies have demonstrated that dopamine stimulates acetylcholine muscarinic receptors on sympathetic ganglion neurons (Libet and Tosaka 1969; Libet and Owman 1974). However, the detailed innervation pattern of SIF cells remains unknown.

Glomus cells in the carotid body and aortic body, which are similar to SIF cells, have been identified as sensors for arterial lower pO_2 and acidity (for a review, see Lahiri et al. 2001). They have been found to make synaptic contacts with the sensory nerve endings of pseudounipolar neurons from the petrosal and nodose ganglia, respectively. ATP is released in the carotid body by hypoxic stimulation and is a candidate for

This study was partly supported by Grants-in-Aid from the Japan Society for the Promotion of Science to T.K. (25350823) and Y.Y. (22580330).

F. Takaki · N. Nakamuta · Y. Yamamoto (✉)
Laboratory of Veterinary Anatomy and Cell Biology, Faculty of Agriculture, Iwate University, 3-18-8 Ueda, Morioka, Iwate 020-8550, Japan
e-mail: yyoshio@iwate-u.ac.jp

T. Kusakabe
Laboratory for Anatomy and Physiology, Department of Sport and Medical Science, Kokushikan University, Tama, Tokyo 206-8515, Japan

being the major excitatory transmitter from glomus cells to sensory nerve endings (Nurse and Piskuric 2013). Immunohistochemistry has revealed that sensory nerve endings immunoreactive for P2X2 and P2X3 purinoreceptors are located around glomus cells in the carotid and aortic bodies (Prasad et al. 2001; Piskuric et al. 2011). Ultrastructural observations have shown both efferent and afferent nerve terminals on SIF cells (Kondo 1977; Matthews and Raisman 1969) and catecholamine contents in sympathetic ganglia have been found to be enhanced under hypoxic conditions (Borghini et al. 1994; Dalmaz et al. 1988, 1993). Thus, sympathetic SIF cells might also be innervated by P2X2- and/or P2X3-expressing sensory nerve endings. Although a previous study reported that vagal sensory nerve fibers immunoreactive for substance P and calcitonin gene-related peptide are distributed in the superior ganglion (Zeidi and Matthews 2013), P2X purinoreceptors containing sensory nerve endings have not as yet been identified.

In order to reconsider the neural circuits in the superior cervical ganglion, attempt here to demonstrate the morphological interrelationship between SIF cells, preganglionic nerve endings and postganglionic cells by using multilabeling immunofluorescence with antibodies against TH for SIF cells, DBH for postganglionic cells and the vesicular acetylcholine transporter (VAChT) for preganglionic fibers. Immunohistochemistry for P2X3 is performed with a focus on the relationship between nerve endings and SIF cells in order to demonstrate sensory innervation. We also perform retrograde neurotracing with fast blue (FB) dye to identify the origin of nerve endings in the superior cervical ganglion.

Materials and methods

Animals

Eight-week-old male Wistar rats (Japan SLC, Hamamatsu, Japan) were used. All procedures for animal handling were performed in accordance with the guidelines of the local Animal Ethics Committee of Iwate University (accession number: A201329).

Immunohistochemistry

Fifteen rats were used for immunohistochemistry. Each rat was anesthetized by an intraperitoneal injection of pentobarbital sodium (55 mg/kg) and transcardially perfused through the ascending aorta with Ringer's solution (300 ml) followed by 4 % paraformaldehyde in 0.1 M phosphate buffer (pH 7.4; 300 ml). The superior cervical ganglia were removed and further fixed with the same fixative for 3–5 h at 4 °C. In some animals, the stellate ganglion, celiac ganglion and pelvic ganglion were also fixed for comparisons. Tissues were then rinsed in phosphate-buffered saline (PBS, pH 7.4), soaked in 30 % sucrose in PBS and frozen with O.C.T. compound medium (Sakura Finetek, Tokyo, Japan). The tissues were serially sectioned at a thickness of 10 μm by using a cryostat (CM 1900, Leica, Wetzlar, Germany) and mounted on glass slides coated with chrome alum-gelatin.

The sections were stained by double- or triple-immunofluorescence. They were first incubated for 30 min with non-immune donkey serum (1:50) and then incubated overnight at 4 °C with a mixture of primary antibodies raised against TH and other neurological markers: vesicular acetylcholine transporter (VAChT), DBH, bassoon, dopamine D2 receptor (D2R) and P2X3 (Table 1). Bassoon is a presynaptic active-zone protein that is used as a marker for exocytosis (Schoch and Gundelfinger 2006). Details of antibody combinations are summarized in Table 2. After being incubated with primary antibodies, sections were then treated with a mixture of secondary antibodies for 90 min at 20 °C. They were counterstained with DAPI (4,6-diamidino-2-phenylindole) and coverslipped with Fluoromount (Diagnostic Biosystems, Pleasanton, Calif., USA). As a negative immunohistochemical control, PBS or non-immune serum was used instead of primary or secondary antisera. The specificities of antibodies against D2R and P2X3 were also verified by the preabsorption control.

A polyclonal rabbit antibody for D2R was raised against a synthetic polypeptide of 270–370 amino acid residues of mouse D2R (Narushima et al. 2006). The D2R antibodies were used in an immunohistochemical analysis of brain tissue (Narushima et al. 2006; Uchigashima et al. 2007). Control peptide was pre-incubated at the final concentration of the antigen peptide (1 mg/mg) overnight at 4 °C. Then, sections were stained by using immunofluorescence as mentioned above. On the other hand, a polyclonal rabbit antibody for P2X3 was raised against a synthetic polypeptide of 383–397 amino acid residues of rat P2X3 (VEKQSTDSGAYSIGH). This antibody was widely used in the immunohistochemistry of peripheral nervous ganglia (e.g., Huang et al. 2011; Fan et al. 2014). To perform pre-absorption tests, antibody was incubated with control peptide (1 mg/ml) overnight at 4 °C. Then, sections of superior cervical ganglion and carotid body were stained by immunofluorescence as mentioned above. Because numerous P2X3 nerve endings have been reported in the carotid body (Prasad et al. 2001), we also used sections of carotid body.

Observations

Sections were examined with a confocal scanning laser microscope (C1, Nikon, Tokyo, Japan). Images of Alexa488, Cy3 and Alexa647 were colored in green, red and white by using computer software (NIS-element, Nikon). The Z-stacks

Table 1 Antibodies used. The antibody numbers in this table are also employed in Table 2. Sources: *A* Cell Signaling Technology (Danvers, Mass., USA); *B* Merck Millipore (Billerica, Mass., USA); *C* Enzo Life Science (Farmingdale, N.Y., USA); *D* Frontier Sciences (Sapporo, Japan); *E* Neuromics (Edina, Minn., USA); *F* Jackson ImmunoResearch (West Grove, Pa., USA); *G* Invitrogen (Carsbad, Calif., USA)

Antibody ID	Enzyme	Abbreviation	Host	Code	Clone number	Dilution	Source
Primary antibodies							
1	Tyrosine hydroxylase	TH	Rabbit	2792		1:200	A
2	Tyrosine hydroxylase	TH	Mouse	MAB318	LNC1	1:1000	B
3	Dopamine β-hydroxylase	DBH	Mouse	MAB308	4 F10.2	1:4000	B
4	Vesicular acetylcholine transporter	VAChT	Goat	BML-SA109		1:5000	C
5	Bassoon		Mouse	ADI-VAM-PS003-D	SAP7F407	1:5000	C
6	Dopamine D2 receptor	D2R	Rabbit	D2R-Rb-Af750-1		1:200	D
7	P2X3 receptor	P2X3	Rabbit	RA10109		1:4000	E
Secondary antibodies							
a	Alexa488-labeled anti-mouse IgG		Donkey	715-545-150		1:200	F
b	Alexa488-labeled anti-rabbit IgG		Donkey	711-545-152		1:200	F
c	Cy3-labeled anti-rabbit IgG		Donkey	711-165-152		1:100	F
d	Cy3-labeled anti-goat IgG		Donkey	705-165-147		1:100	F
e	Cy3-labeled anti-guinea Pig IgG		Donkey	706-165-148		1:100	F
f	Cy3-labeled anti-mouse IgG		Donkey	715-165-151		1:100	F
g	Alexa647-labeled anti-goat IgG		Donkey	A21447		1:1000	G

of confocal projection images were made from 5–15 series of images at 0.5- to 1-μm intervals, in the same software. Some images were also reconstructed to provide a three-dimensional view from intact or binary images that were converted from the original.

Retrograde labeling

Three rats were anesthetized with pentobarbital (15 mg/kg; intraperitoneal injection) and the neck of each was incised to expose the left superior cervical ganglion. A small incision was made on the surface of the ganglion and 200 nl of a retrograde tracer (2.5 % FB dye in 10 % dimethylsulfoxide; Polysciences, Warrington, Pa., USA) was then injected by using a thin glass micropipette connected to a microinjector (IM-9B, Narishige, Tokyo, Japan). After survival for 5 days, animals were fixed by transcardial perfusion as described above. The petrosal, jugular and nodose ganglia and dorsal root ganglia at C1-C3 were dissected out. Serial 10-μm sections were immunostained for P2X3. Epifluorescence microscopy (Eclipse 80i, Nikon, Tokyo) was used to count FB-labeled neurons. Furthermore, 50-μm sections of the spinal cord at Th1 to Th3 were examined. Some sections were photographed by using a confocal scanning laser microscope.

Results

Immunohistochemical characteristics of SIF cells

SIF cells in the superior cervical ganglion showed intense immunoreactivity for TH (Fig. 1). These cells were approximately 8–15 μm in diameter and were oval or polygonal in shape. Some possessed thin cytoplasmic processes. Although SIF cells were mostly gathered into clusters, some solitary cells were also observed in intraganglionic nerve bundles. DBH immunoreactivity was observed in ganglionic cell

Table 2 Combinations of antibodies for multilabeling immunofluorescence. *Numbers* and *letters* are as shown in Table 1

Combination	Primary antibody 1	Secondary antibody 1	Primary antibody 2	Secondary antibody 2	Primary antibody 3	Secondary antibody 3
TH/DBH/VAChT	1	c	3	a	4	g
TH/Bassoon	1	c	5	a		
TH/D2R	2	a	7	e		
TH/P2X3/VAChT	2	f	8	b	4	g
TH/P2X3	2	f	8	b		

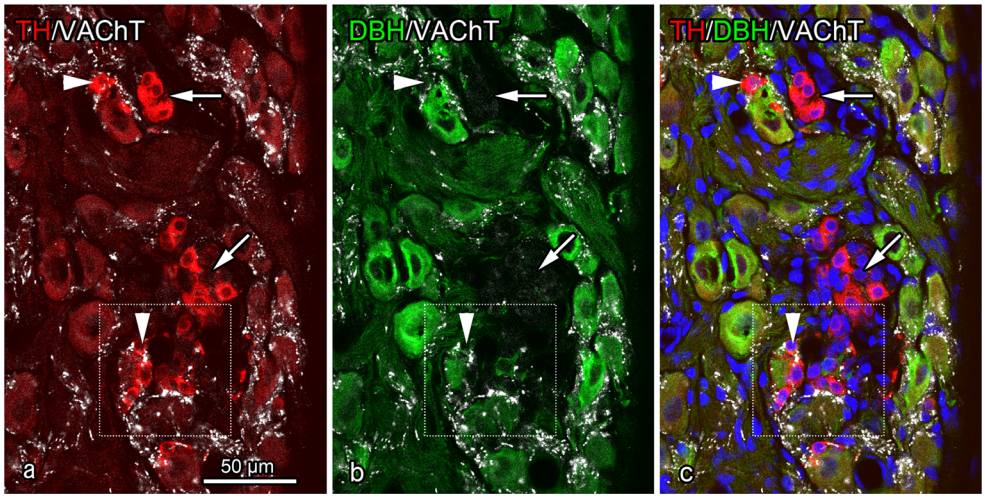

Fig. 1 Low magnification views of SIF cells in the superior cervical ganglion as revealed by triple-immunolabeling for tyrosine hydroxylase (*TH*; Cy-3, *red*), dopamine β-hydroxylase (*DBH*; Alexa488, *green*) and vesicular acetylcholine transporter (*VAChT*; Alexa647, *white*). **a** Merged image of TH and VAChT immunoreactivity. **b** Merged image of DBH and VAChT immunoreactivity. **c** Merged image of the three antibodies. SIF cells with intense immunoreactivity for TH are clustered between ganglionic cells. VAChT-immunoreactive puncta were observed on the cellular surface of some SIF cells (*arrowheads*) but not on others (*arrows*). Almost all SIF cells lacked immunoreactivity for DBH and only a few cells were immunoreactive. *Dotted rectangles* in **a–c** are enlarged in Fig. 2a-c. Nuclei are stained by DAPI (*blue*) in **c**

bodies, nerve fibers and a few SIF cells; however, most SIF cells were not immunoreactive for DBH (Figs. 1, 2a-c). Some TH-immunoreactive SIF cells were closely attached to DBH-immunoreactive ganglionic cells (Figs. 1, 2d-f). VAChT immunoreactivity was observed as punctate labeling on SIF and ganglionic cells (Figs. 1, 2). However, VAChT-immunoreactive puncta were not observed on some clusters of SIF cells. In some cases, SIF cells with VAChT-immunoreactive puncta were located in the shallow dimples of flat cytoplasmic processes in ganglionic cells (Fig. 2d-f). On the other hand, the accumulation of dot-like immunoreactive products for bassoon was detected beneath the cellular membranes of SIF cells (Fig. 2g-i). These bassoon-immunoreactive products were observed in both the attachment and opposite sides to ganglionic cells. Immunoreactivity for D2R was observed in both SIF and ganglionic cells (Fig. 3a-c). Preabsorption of anti-D2R antibody with immunogen peptide completely blocked immunostaining in the SIF cells and ganglion cells in superior cervical ganglia (Fig. 3d, e).

Morphology of P2X3-immunoreactive nerve endings around SIF cells

P2X3-immunoreactive nerve endings were associated with TH-immunoreactive SIF cells (Fig. 4). P2X3-immunoreactive nerve endings were attached to SIF cells with or without VAChT-immunoreactive puncta. Nerve endings that were immunoreactive for P2X3 originated from thick nerve fibers (approximately 2 μm in diameter), were branched and terminated on SIF cells (Fig. 5). The axon terminals of the P2X3-immunoreactive nerve endings were hederiform and flat. Small terminals were attached to SIF cells and large terminals ensheathed around SIF cells. A three-dimensional reconstruction confirmed that the axon terminals of nerve endings with P2X3 immunoreactivity branched to several neighboring SIF cells and tightly ensheathed SIF cells (Fig. 5c). In the preabsorption control for P2X3 antibody, no immunoreactive products were observed in the superior cervical ganglion, carotid body and petrosal ganglion (not shown).

Innervation of SIF cells

Triple-immunolabeling for TH, P2X3 and VAChT revealed various innervation patterns for SIF cells (Fig. 6). Some clusters of SIF cells exhibited VAChT-immunoreactive puncta, whereas no P2X3-immunoreactive endings were associated with them (Fig. 6d). In other clusters, only flattened nerve endings with P2X3 immunoreactivity were found around the cells (Fig. 6e). Moreover, the other clusters exhibited distributions of both VAChT-immunoreactive puncta and P2X3-immunoreactive nerve endings (Fig. 6f). Therefore, the patterns of innervation on SIF cells could be divided into three types: (1) with only VAChT-immunoreactive puncta, (2) with only P2X3-immunoreactive nerve endings, (3) with both VAChT-immunoreactive puncta and P2X3-immunoreactive nerve endings.

Retrograde tracer study

After the injection of FB retrograde tracer into the superior cervical ganglion, labeled neurons were observed in the ipsilateral sensory ganglia of the glossopharyngeal and vagus

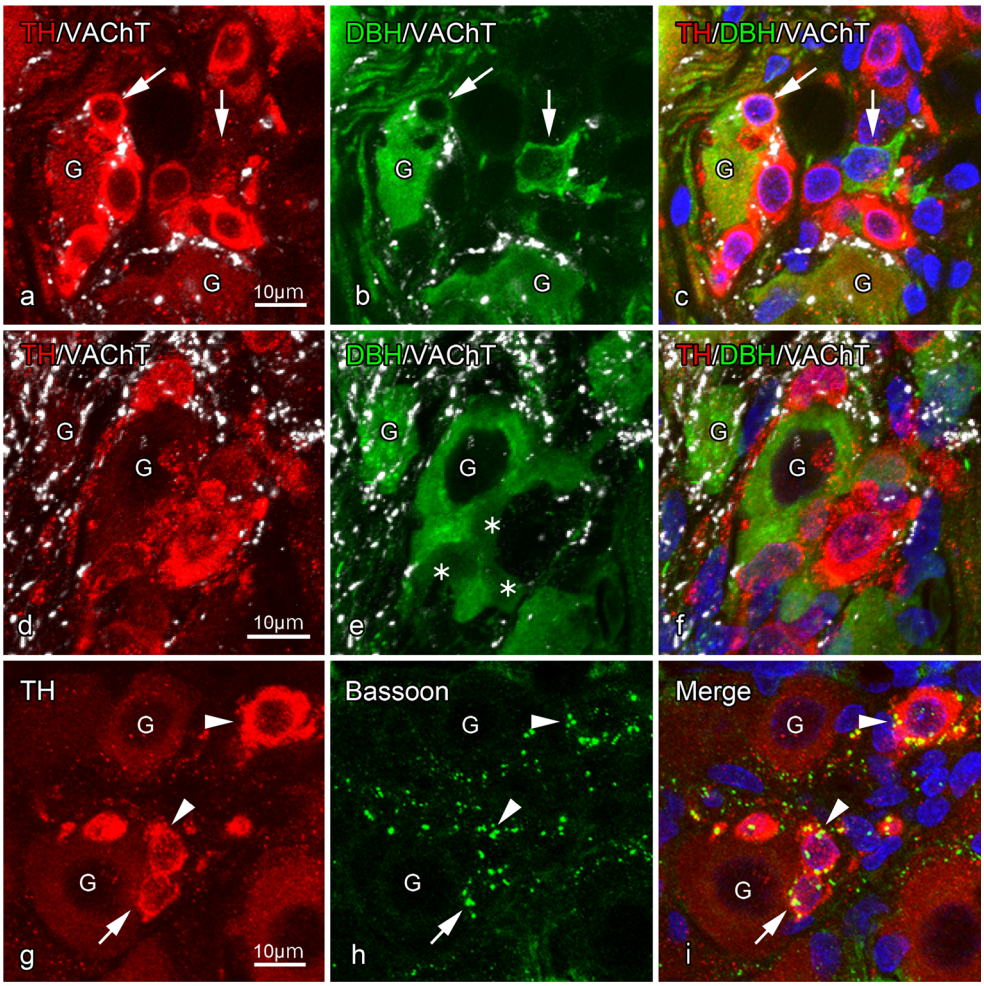

Fig. 2 **a–c** TH- and DBH-immunoreactive SIF cells. Most SIF cells are intensely immunoreactive for TH and two cells shown here are also immunoreactive for DBH. Some SIF cells are closely apposed to ganglionic cells (*G*). **d–f** SIF cells around a ganglionic cell. SIF cells with VAChT-immunoreactive puncta are located in the dimples of flat cytoplasmic processes (*asterisks*). **g–i** Bassoon-immunoreactive products are observed beneath the cellular membrane near the ganglionic cells (*arrows*). Bassoon immunoreactivity was also observed at the opposite side of the ganglionic cells (*arrowheads*). Nuclei are stained by DAPI (*blue*) in **c**, **f**, **i**

nerves, i.e., petrosal, jugular and nodose ganglia. Some FB-labeled neurons were also immunoreactive for P2X3 (Fig. 7a-c). Based on three experiments, a total of 143, 61 and 6 cells were labeled with FB in the petrosal, jugular and nodose ganglia, respectively. Of these FB-labeled cells, 72 (50.3 %), 8 (13.1 %) and 2 cells (33.3 %) were also immunoreactive for P2X3 (Fig. 7d). In the dorsal root ganglion at C1-C3, only one P2X3-immunoreactive FB-labeled cell was observed among a total of 48 FB-labeled cells in three experiments. The proportions of P2X3-immunoreactive FB-labeled cells were 86.7, 9.6, 2.4 and 1.2 % in the petrosal, jugular, nodose and dorsal root ganglia, respectively (Fig. 7e). Raw data are shown in Table 3. In the spinal cord at the Th1-Th3 levels, FB-labeled neurons were observed in the mediolateral nucleus (Fig. 7f).

Stellate ganglion, celiac ganglion and pelvic ganglion

In the stellate, celiac and pelvic ganglia, SIF cells with TH immunoreactivity were clustered between ganglion nerve cells, as in the superior cervical ganglia. VAChT-immunoreactive puncta were distributed on the SIF cells in these ganglia but no P2X3-immunoreactive nerve endings were present (Fig. 8).

Discussion

SIF cells as interneurons in superior cervical ganglion

The close relationship among SIF cells, VAChT-immunoreactive preganglionic nerve fibers and DBH-immunoreactive postganglionic cells suggests that SIF cells in the superior cervical ganglia play a role as interneurons, as previously reported. Because few SIF cells with DBH immunoreactivity were observed in a previous study (Heym et al. 1993), dopamine might be the main transmitter of SIF cells. The presence of bassoon-immunoreactive products beneath the cellular membrane in TH-immunoreactive SIF cells suggests that SIF cells release dopamine to the postganglionic nerve cell body. Furthermore, dopamine released from SIF cells might bind to D2R on ganglionic cells to modulate their excitability. Both D1R and D2R mRNAs have been shown to

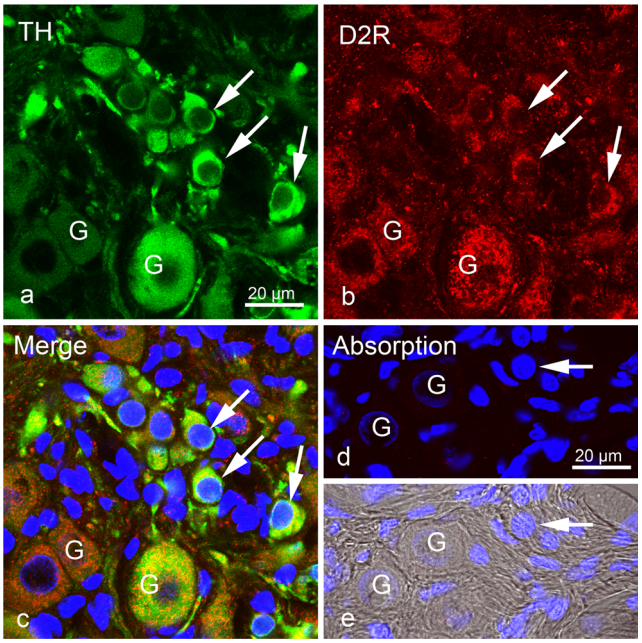

Fig. 3 Distribution of dopamine receptors D2 (*D2R*). **a–c** D2R immunoreactivity is observed in both SIF cells and ganglionic cells. **d** No immunoreactivity is found in SIF cells (*arrow*) and ganglion cells (*G*) in the preabsorption control. **e** Differential interference contrast image with DAPI nuclear staining (*blue*) of the same section as in **d**

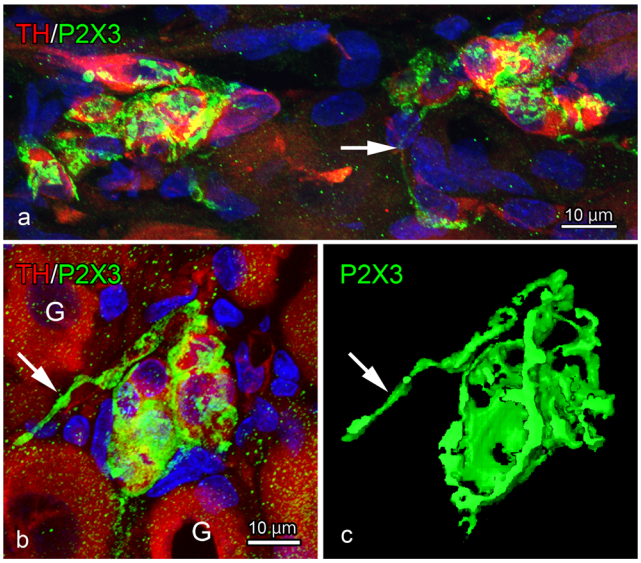

Fig. 5 Double-immunolabeling for TH and P2X3 in the rat superior cervical ganglion. **a** Two P2X3-immunoreactive nerve endings associate with SIF cell clusters. A P2X3-immunoreactive thick axon (*arrow*) was observed near the SIF cell cluster *right* (*arrow*). **b** Projection view of flattened axon terminals. P2X3-immunoreactive axon terminals are wrapped around the cluster of SIF cells (*arrow* parent axon of the nerve ending). **c** Three-dimensional reconstruction of the P2X3-immunoreactive axon terminal in **b**. Nuclei of cells are revealed by DAPI (*blue*) in **a**, **b** (*G* ganglionic cells)

be expressed in the superior cervical ganglia of rabbits (Bairam et al. 2003), whereas only D2R mRNA has been detected in the ganglionic cells of rats (Czyzyk-Krzeska et al. 1992). With regard to function, Brokaw and Hansen (1987) reported that the D2R antagonist, spiroperidol, induces the synthesis of noradrenaline in the rat superior cervical ganglion. Thus, ganglionic cells in the superior cervical ganglion are regulated by the dopamine released from SIF cells via D2R.

Previous studies have reported that axon terminals make synapses with SIF cells in both directions (Case and Matthews 1985; Kondo 1977; Matthews and Raisman 1969). Therefore, SIF cells might regulate preganglionic fibers that are immunoreactive to VAChT and also postganglionic cells that are immunoreactive to DBH by using synaptic transmission. In addition to synaptic regulation, dopamine has been shown to regulate neuronal function by volume transmission in the

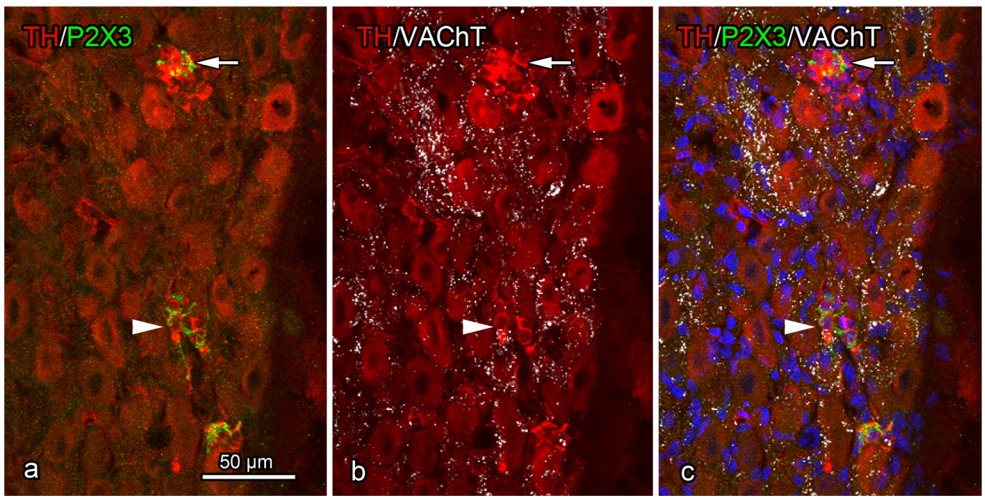

Fig. 4 Low magnification view of P2X3-immunoreactive nerve endings in the superior cervical ganglion as revealed by triple-immunolabeling for TH (Cy-3, *red*), P2X3 (Alexa488, *green*) and VAChT (Alexa647, *white*). **a** Merged image of TH and P2X3 immunoreactivity. **b** Merged image of TH and VAChT immunoreactivity. **c** Merged image from the three antibodies. P2X3-immunoreactive nerve endings associate with clusters of SIF cells without (*arrows*) and with (*arrowheads*) VAChT-immunoreactive puncta. Nuclei are stained by DAPI (*blue*) in **c**

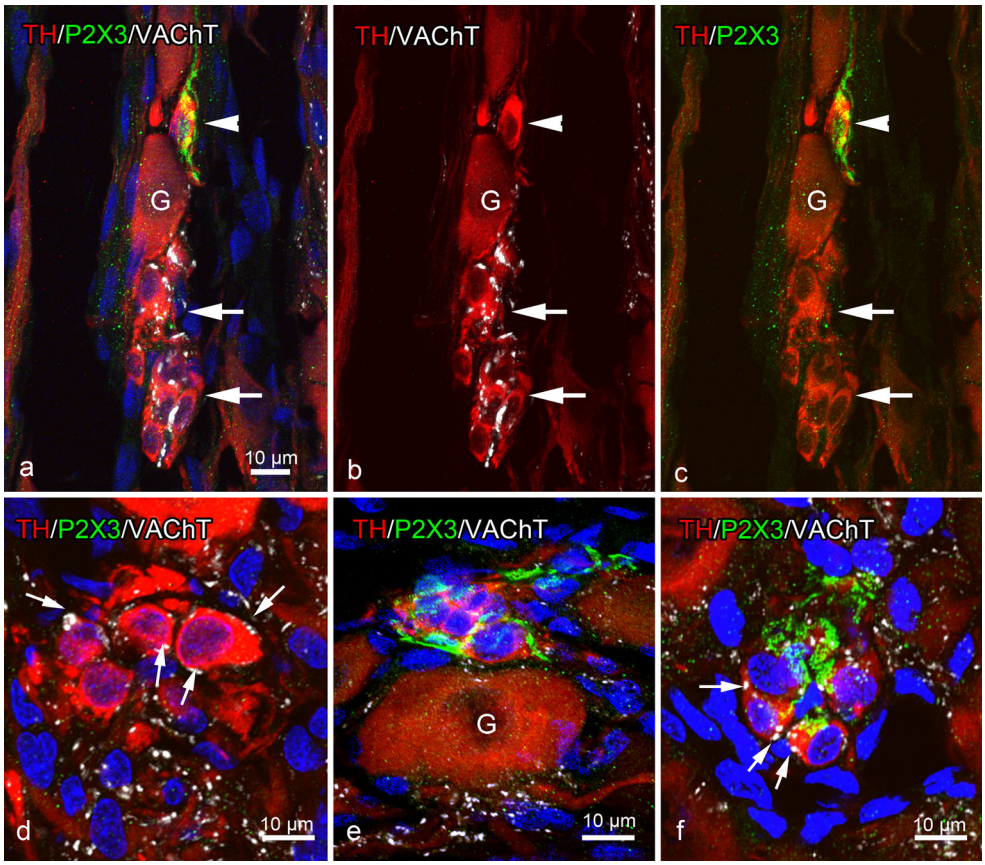

Fig. 6 Innervation patterns on SIF cells in the superior cervical ganglia (*G* ganglionic cells). **a–c** Only P2X3-immunoreactive nerve endings are found on an SIF cell (*arrowhead*), whereas only VAChT-immunoreactive puncta are detected on SIF cells in the cluster (*arrows*). **d** SIF cells with VAChT-immunoreactive puncta (*arrows*) and without P2X3-immunoreactive nerve endings. **e** High-power view of TH-immunoreactive SIF cells with P2X3-immunoreactive nerve endings and without VAChT-immunoreactive puncta (*arrows*). **f** SIF cells with both P2X3-immunoreactive nerve endings and VAChT-immunoreactive puncta (*arrows*)

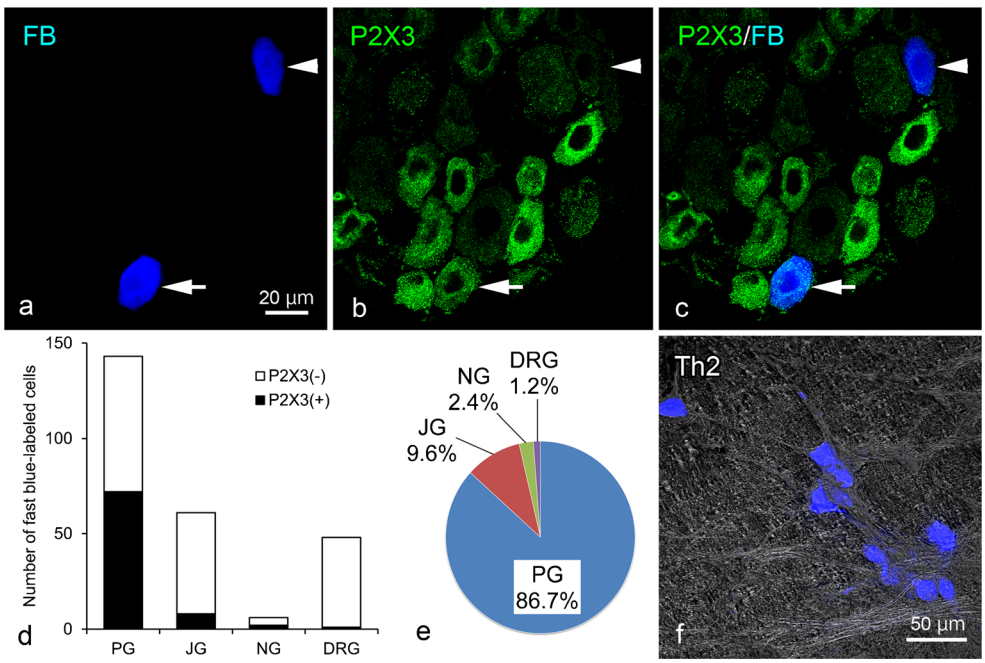

Fig. 7 Fast-blue (*FB*)-labeled ganglionic cells after their injection into superior cervical ganglion. **a–c** Two FB-labeled cells are visible in the petrosal ganglion; one cell is also immunoreactive for P2X3 (*arrow*), whereas the other cell is not (*arrowhead*). **c** Merged image of **a**, **b**. **d** Total number of FB-labeled cells in the petrosal ganglion (*PG*), jugular ganglion (*JG*), nodose ganglion (*NG*) and dorsal root ganglion (*DRG*) at the levels of C1-C3 from three experiments. *Closed* and *open columns* show P2X3-immunoreactive and P2X3-negative cells, respectively. **e** Percentages of FB-labeled P2X3-immunoreactive neurons in PG, JG, NG and DRG. A total of 86.7 % of cells was detected in the PG. **f** FB-immunoreactive cells in the lateral reticular nucleus on the ipsilateral side of the spinal cord at the Th2 level

Table 3 Number of fast-blue-labeled cells after injection of dye into superior cervical ganglion given as P2X3-positive labeled cells divided by total number of labeled cells (*PG* petrosal ganglion, *JG* jugular ganglion, *NG* nodose ganglion, *DRG* dorsal root ganglion, *ND* not detected)

Animal number	PG	JG	NG	DRG (C1-C3)
1	31/35	7/42	ND	0/7
2	25/62	0/7	2/6	ND
3	16/46	1/12	ND	1/41
Total	72/143	8/61	2/6	1/48

central nervous system (Fuxe et al. 2010). The localization of bassoon-immunoreactive vesicle-releasing sites on the opposite site of postganglionic cells implies that dopamine is released into the extrasynaptic region from SIF cells. Thus, dopamine released from SIF cells might regulate postganglionic cells by both synaptic and volume transmissions. Furthermore, D2R immunoreactivities have been observed in SIF cells, suggesting the feedback regulation of SIF cells themselves in an autocrine/paracrine manner.

Sensory nerve endings around SIF cells

The present investigation has revealed that some of the SIF cells in the superior cervical ganglion receive P2X3-immunoreactive afferent nerve endings associated with the SIF cell cluster and that synaptic contact might occur between nerve endings and SIF cells. Previous studies have reported that nerve endings with P2X2 and P2X3 immunoreactivities are distributed around the cluster of glomus cells in the carotid and aortic bodies (Prasad et al. 2001; Piskuric et al. 2011). In the neuroepithelial body in the mouse lung, ramified nerve endings with P2X2 and/or P2X3 immunoreactivities have been found to be distributed between sensory cells (Brouns et al. 2009). Furthermore, nerve endings with P2X2 and P2X3 immunoreactivities are associated with taste cells in lingual taste buds (Kataoka et al. 2006; Yang et al. 2012). The relationship between SIF cells and P2X3-immunoreactive nerve endings is similar to that of other sensory cell-nerve complexes. Physiological experiments have revealed that ATP is probably one of the main transmitters for signal transmissions from glomus cells to afferent nerve endings (Nurse and Piskuric 2013) and from taste cells to gustatory nerves (Roper 2013). Moreover, studies by using microbiosensors on the whole carotid body or glomus cell culture with bioluminescence detection have revealed that hypoxic stimulation induces the release of ATP with dopamine from glomus cells (Buttigieg and Nurse 2004; Masson et al. 2008). In physiological experiments with an ATP-sensitive biosensor, type II gustatory cells have been shown to release ATP via pannexin 1 hemichannels when taste stimuli are applied (Huang et al. 2007). SIF cells in the superior cervical ganglia might therefore release ATP and dopamine when cells are depolarized and this ATP might bind to P2X purinoreceptors in sensory nerve endings.

Innervation of SIF cells

The results of the retrograde tracer experiment indicate that most sensory nerve endings with P2X3 immunoreactivity in the superior cervical ganglion are derived from the petrosal ganglion. McDonald (1983) suggested, based on histological observations, that sensory nerve fibers in the carotid sinus nerve project to the superior cervical ganglion via communicating branches. P2X3-immunoreactive nerve endings might run through the carotid sinus nerve. A previous study demonstrated that VAChT can be used as an immunohistochemical marker of cholinergic nerve terminals (Schäfer et al. 1998). In the present study, we confirmed that neurons in the mediolateral nucleus of the spinal cord at Th1-Th3 project to the superior cervical ganglion in our retrograde tracing experiments and that they might also be the origin of VAChT axon terminals in the superior cervical ganglion. Based on the

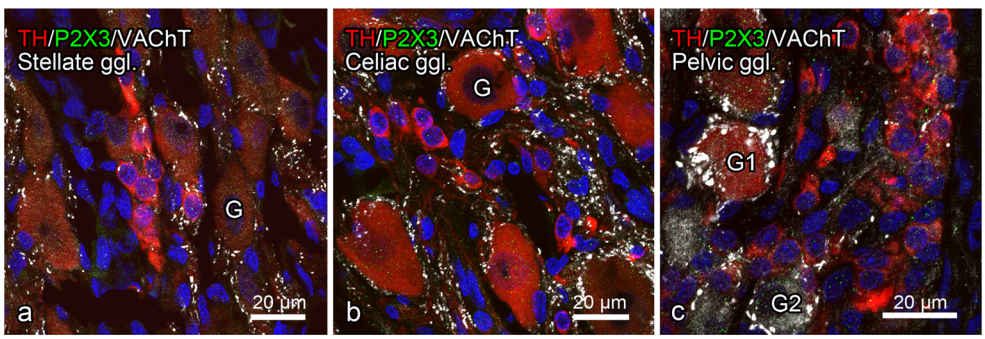

Fig. 8 Triple-labeling for TH (Cy-3, *red*), P2X3 (Alexa488, *green*) and VAChT (Alexa647, *white*) in the stellate ganglion (**a**; *ggl* ganglion), celiac ganglion (**b**) and pelvic ganglion (**c**). No P2X3-immunoreactive nerve endings are detected around the TH-immunoreactive SIF cells in these ganglia and VAChT-immunoreactive puncta are distributed on the cells. Note TH-immunoreactive ganglionic cells (*G*) in **a**, **b** and ganglionic cells with TH and VAChT immunoreactivities (*G1* and *G2*, respectively) in **c**

combination of P2X3- and VAChT-immunoreactivities around SIF cells, SIF cells in the superior cervical ganglion seem to be divided into three subpopulations based on their innervation as shown in Fig. 9: (1) with preganglionic terminals only, (2) with glossopharyngeal sensory nerve endings only, (3) with both sensory nerve endings and preganglionic axon terminals. Preganglionic fibers of both sympathetic and parasympathetic nerves have been reported to be distributed in the carotid body, based on tracer and denervation studies (for a review, see Kummer 1997). On the other hand, Kummer and Neuhuber (1989) classified the clusters of paraganglion cells in the vagus nerve into two types, namely, glomus-like bodies (GLB) and SIF-cell like bodies (SLB); GLB have a cellular capsule emerging from the perineurium but SLB do not. These authors further reported that the enlarged afferent nerve endings are unevenly distributed in GLB but not in SLB. The variations of SIF cells in the superior laryngeal nerve are similar to those of other paraganglia.

Functional considerations

SIF cells with VAChT-immunoreactive puncta and without P2X3-immunoreactive sensory nerve endings might be interneurons between preganglionic nerve terminals and ganglionic neurons. Previous studies have confirmed that SIF cells are interneurons between preganglionic nerve terminals and postganglionic neurons in the sympathetic nervous system (Eränkö 1978; Matthews 1989). Physiological experiments have shown that dopamine stimulates acetylcholine muscarinic receptors on sympathetic ganglion neurons to produce a slow inhibitory postsynaptic potential, s-IPSP (Libet and Owman 1974). In addition to s-IPSP, a slow excitatory postsynaptic potential, s-EPSP, has also been found to be modulated by dopamine (Libet and Tosaka 1969). On the other hand, D2R is known to be generally coupled with the Gαi protein to reduce cAMP concentrations (Beaulieu and Gainetdinov 2011). In the carotid body, dopamine has been shown to be released by hypoxia and by the inhibition of sensory discharge in the carotid sinus nerve (Ituriaga and Alacayaga 2004). Therefore, D2R in the superior cervical ganglion might receive feedback inhibition after the depolarization of SIF cells, as in the glomus cells in the carotid body.

The SIF cells innervated by P2X3-immunoreactive sensory nerve endings might be sensory cells, because synaptic inputs might be absent. After hypoxic exposure (10 % O_2) for 2–28 days, dopamine content increases in rat sympathetic ganglia, including the superior cervical ganglion (Borghini et al. 1994; Dalmaz et al. 1988). Furthermore, the number of TH-immunoreactive SIF cells in the superior cervical and celiac-cranial mesenteric ganglia also increases after hypoxia for 14 days (Dalmaz et al. 1993). These findings suggest that SIF cells in the superior cervical ganglia are involved in the response to hypoxia and also that P2X3 nerve endings transmit the hypoxic responses of SIF cells to the central nervous system. However, P2X3-immunoreactive nerve endings have not been detected around SIF cells in other sympathetic ganglia, including the stellate, celiac and pelvic ganglia. Based on the findings of ontogenetic studies in mutant mice, the

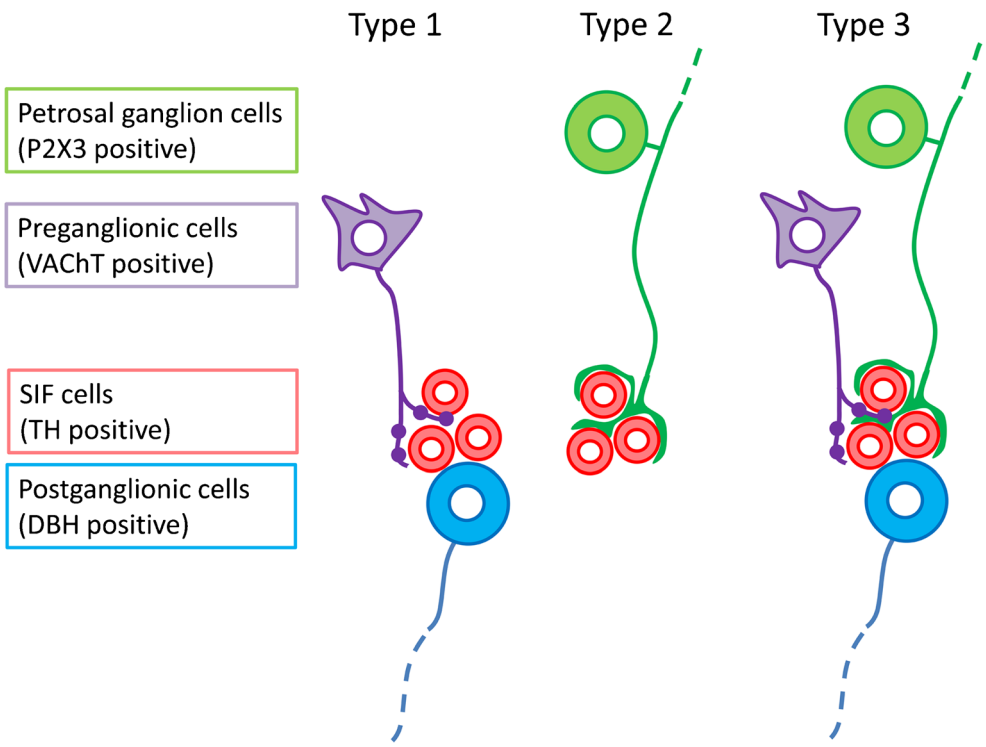

Fig. 9 Three types of SIF cells classified by their innervation. *Type 1* SIF cells with preganglionic terminals only. *Type 2* SIF cells with glossopharyngeal sensory nerve endings only. *Type 3* SIF cells with both sensory nerve endings and preganglionic axon terminals

glomus cells in the carotid body are derived from the superior cervical ganglion (for a review, see Kameda 2014). Furthermore, sensory nerve endings in the carotid body have been shown to be derived from the petrosal ganglionic cells based on the findings of a degeneration study (Hess and Zapta 1972) and on retrograde (Kalia and Davies 1978) and anterograde neuronal tracing (Fidone et al. 1977). Since the sensory endings around SIF cells might be derived from petrosal ganglionic cells as discussed above, the morphological characteristics of SIF cells are similar to those of the glomus cells. SIF cells that associate with P2X3-immunoreactive nerve endings in the superior cervical ganglion might thus be ectopic glomus cells.

SIF cells associated with both P2X3-immunoreactive sensory nerve endings and VAChT-immunoreactive preganglionic terminals appear to act as an interconnection between preganglionic and primary sensory neurons. Previous studies have reported that hypoxic and/or hypercapnic stimuli evoke sympathetic activity in the cervical trunk of the sympathetic nerve, renal sympathetic nerve and splanchnic nerve (Huang et al. 1988; Hirakawa et al. 1997; Moreira et al. 2006). This type of cell might monitor both preganglionic nerve activity and hypoxia in the arterial blood and might also be involved in the feedback regulation of sympathetic activity.

Concluding remarks

SIF cells in the superior cervical ganglion are innervated by preganglionic fibers and glossopharyngeal sensory nerve endings and can be classified into three types. These cells might have sensory functions in addition to their role as interneurons and might regulate sympathetic nerves. Since the neural circuit in the superior cervical ganglion is highly complex, as reported in the present study, the exact function of each type of SIF cell should be examined in more detail in future studies.

References

Bairam A, Carroll JL, Labelle Y, Khandjian EW (2003) Differential changes in dopamine D2- and D1-receptor mRNA levels induced by hypoxia in the arterial chemoreflex pathway organs in one-day-old and adult rabbits.Biol Neonate 84:222–231

Beaulieu J-M, Gainetdinov RR (2011) The physiology, signaling, and pharmacology of dopamine receptors. Pharmacol Rev 63:182–217

Borghini N, Dalmaz Y, Peyrin L, Heym C (1994) Chemosensitivity, plasticity, and functional heterogeneity of paraganglionic cells in the rat coelic-superior mesenteric complex. Microsc Res Tech 29: 112–119

Brokaw JJ, Hansen JT (1987) Evidence that dopamine regulates norepinephrine synthesis in the rat superior cervical ganglion during hypoxic stress. J Auton Nerv Syst 18:185-193

Brouns I, Oztay F, Pintelon I, De Proost I, Lembrechts R, Timmermans JP, Adriaensen D (2009) Neurochemical pattern of the complex innervation of neuroepithelial bodies in mouse lungs. Histochem Cell Biol 131:55–74

Buttigieg J, Nurse CA (2004) Detection of hypoxia-evoked ATP release from chemoreceptor cells of the rat carotid body. Biochem Biophys Res Commun 322:82–87

Case CP, Matthews MR (1985) A quantitative study of structural features, synapses and nearest-neighbour relationships of small, granule-containing cells in the rat superior cervical sympathetic ganglion at various adult stages. Neuroscience 15:257–282

Czyzyk-Krzeska MF, Lawson EE, Millhorn DE (1992) Expression of D2 dopamine receptor mRNA in the arterial chemoreceptor afferent pathway.J Auton Nerv Syst 41:31–39

Dalmaz Y, Pequignot J-M, Tavitian E, Corttet-Emard J-P, Peyrin L (1988) Long-term hypoxia increases the turnover of dopamine but not norepinephrine in rat sympathetic ganglia. J Auton Nerv Syst 24: 57–64

Dalmaz Y, Borghini N, Pequignot JM, Peyrin L (1993) Presence of chemosensitive SIF cells in the rat sympathetic ganglia: a biochemical, immunocytochemical and pharmacological study. Adv Exp Med Biol 337:393-399

Eränkö O (1978) Small intensely fluorescent (SIF) cells and nervous transmission in sympathetic ganglia. Ann Rev Pharmacol Toxicol 18:417–430

Fan L, Guan X, Wang W, Zhao J-Y, Zhang H, Tiwari V, Hoffman PN, Li M, Tao Y-X (2014) Impaired neuropathic pain and preserved acute pain in rats overexpressing voltage-gated potassium channel subunit Kv1.2 in primary afferent neurons. Mol Pain 10:8

Fidone SJ, Zapata P, Stensaas LJ (1977) Axonal transport of labeled material into sensory nerve ending of cat carotid body. Brain Res 124:9–28

Fuxe K, Dahlström AB, Jonsson G, Marcellino D, Guescini M, Dam M, Manger P, Agnati L (2010) The discovery of central monoamine neurons gave volume transmission to the wired brain. Prog Neurobiol 90:82–100

Hess A, Zapta P (1972) Innervation of the cat carotid body: normal and experimental studies. Fed Proc 31:1365–1382

Heym C, Common B, Yin S, Klimaschewski L, Couraud J-Y, Bachmann S (1993) Neurochemistry, connectivity and plasticity of small intensely fluorescent (SIF) cells in the rat superior cervical ganglion. Ann Anat 175:309–319

Heym C, Klimaschewski L, Borghini N, Fischer-Colbrie R (1994) Immunohistochemistry of small intensely fluorescent (SIF) cells and of SIF cell-associated nerve fibers in the rat superior cervical ganglion. Microsc Res Tech 29:143–150

Hirakawa H, Nakamura T, Hayashida Y (1997) Effect of carbon dioxide on autonomic cardiovascular responses to systemic hypoxia in conscious rats. Am J Physiol 273:R747–R754

Huang B, Zhao X, Zheng L-B, Zhang L, Ni B, Wang YW (2011) Different expression of tissue inhibitor of metalloproteinase family members in rat dorsal root ganglia and their changes after peripheral nerve injury. Neuroscience 193:421–428

Huang W, Lahiri S, Mokashi A, Sherpa AK (1988) Relationship between sympathetic and phrenic nerve responses to peripheral chemoreflex in the cat. J Auton Nerv Syst 25:95–105

Huang YJ, Maruyama Y, Dvoryanchikov G, Pereira E, Chaudhari N, Roper SD (2007) The role of pannexin 1 hemichannels in ATP release and cell-cell communication in mouse taste buds. Proc Natl Acad Sci U S A 104:6436–6441

Huber K (2006) The sympathoadrenal cell lineage: specification, diversification, and new perspectives. Dev Biol 298:335–343

Itturiaga R, Alacayaga J (2004) Neurotransmission in the carotid body: transmitters and modulators between glomus cells and petrosal ganglion nerve terminals. Brain Res Rev 47:46–53

Kalia M, Davies RO (1978) A neuroanatomical search for glossopharyngeal efferents to the carotid body using the retrograde transport of horseradish peroxidase. Brain Res 149:477–481

Kameda Y (2014) Signaling molecules and transcription factors involved in the development of the sympathetic nervous system, with special emphasis on the superior cervical ganglion. Cell Tissue Res 357: 527–548

Kataoka S, Toyono T, Seta Y, Toyoshima K (2006) Expression of ATP-gated P2X3 receptors in rat gustatory papillae and taste buds. Arch Histol Cytol 69:281–288

Kondo H (1977) Innervation of SIF cells in the superior cervical and nodose ganglia: an ultrastructural study with serial sections. Biol Cell 30:253–264

Kummer W (1997) Innervation of paraganglia. In: Unsicker K (ed) Autonomic-endocrine interactions. Taylor & Francis, London, pp 315–356

Kummer W, Neuhuber WL (1989) Vagal paragnglia of the rat. J Electron Microsc Tech 12:343–355

Lahiri S, Rozanov C, Roy A, Storey B, Buerk DG (2001) Regulation of oxygen sensing in peripheral arterial chemoreceptors. Int J Biochem Cell Biol 33:755–774

Libet B, Owman C (1974) Concomitant changes in formaldehyde-induced fluorescence of dopamine interneurones and in slow inhibitory post-synaptic potentials of the rabbit superior cervical ganglion, induced by stimulation of the preganglionic nerve or by a muscarinic agent. J Physiol (Lond) 237:635–662

Libet B, Tosaka T (1969) Slow inhibitory and excitatory postsynaptic responses in single cells of mammalian sympathetic ganglia. J Neurophysiol 32:43–50

Masson JF, Kranz C, Mizaikoff B, Gauda EB (2008) Amperometric ATP microbiosensors for the analysis of chemosensitivity at rat carotid bodies. Anal Chem 80:3991–3998

Matthews MR (1989) Small, intensely fluorescent cells and the paraneuron concept. J Electron Microsc Tech 12:408–416

Matthews MR, Raisman G (1969) The ultrastructure and somatic efferent synapses of small granule-containing cells in the superior cervical ganglion. J Anat 105:255–282

McDonald DM (1983) Morphology of the rat carotid sinus nerve. I. Course, connections, dimensions and ultrastructure. J Neurocytol 12:345–372

Moreira TS, Takakura AC, Colombari E, Guyenet PG (2006) Central chemoreceptors and sympathetic vasomotor outflow. J Physiol (Lond) 577:369–386

Narushima M, Uchigashima M, Hashimoto K, Watanabe M, Kano M (2006) Deporalization-induced suppression of inhibition mediated by endocannabinoids at synapses from fast-spiking interneurons to medium spiny neurons in the striatum. Eur J Neurosci 24:2246–2252

Nurse CA, Piskuric NA (2013) Signal processing at mammalian carotid body chemoreceptors. Semin Cell Dev Biol 24:22–30

Piskuric NA, Vollmer C, Nurse CA (2011) Confocal immunofluorescence study of rat aortic body chemoreceptors and associated neurons in situ and in vitro. J Comp Neurol 519:856–873

Prasad M, Fearon IM, Zhang M, Laing M, Vollmer C, Nurse CA (2001) Expression of P2X3 receptor subunits in rat carotid body afferent neurones: role in chemosensory signalling. J Physiol (Lond) 537: 667–677

Prud'homme MJ, Houdeau E, Serghini R, Tillet Y, Schemann M, Rousseau JP (1999) Small intensely fluorescent cells of the rat paracervical ganglion synthesize adrenaline, receive afferent innervation from postganglionic cholinergic neurones, and contain muscarinic receptors. Brain Res 821:141–149

Roper SD (2013) Taste buds as peripheral chemosensory processors. Semin Cell Dev Biol 24:71–79

Schäfer MK, Eiden LE, Weihe E (1998) Cholinergic neurons and terminal fields revealed by immunohistochemistry for the vesicular acetylcholine transporter. II. The peripheral nervous system. Neuroscience 84:361–376

Schoch S, Gundelfinger ED (2006) Molecular organization of the presynaptic active zone. Cell Tissue Res 326:379–391

Shtukmaster S, Schier MC, Huber K, Krispin S, Kalcheim C, Unsicker K (2013) Sympathetic neurons and chromaffin cells share a common progenitor in the neural crest in vivo. Neural Dev 8:12

Uchigashima M, Narushima M, Fukaya M, Katona I, Kano M, Watanabe M (2007) Subcellular arrangement of molecules for 2-arachidonoylglycerol-mediated retrograde signaling and its hysiological contribution to synaptic modulation in the striatum. J Neurosci 27:3663–3676

Yang R, Montoya A, Bond A, Walton J, Kinnamon JC (2012) Immunocytochemical analysis of P2X2 in rat circumvallate taste buds. BMC Neurosci 13:51

Zeidi ZF, Matthews MR (2013) Source and origin of nerve fibers immunoreactive for substance P and calcitonin gene-related peptide in the normal and chronically denervated superior cervical sympathetic ganglion of the rat. Auton Neurosci 173:28–38